

Adaptive low-rank approximation and denoised Monte-Carlo approach for high-dimensional Lindblad equations

C. Le Bris,¹ P. Rouchon,^{2,*} and J. Roussel¹

¹*École des Ponts and Inria, 6 et 8 avenue Blaise Pascal, 77455 Marne-La-Vallée Cedex 2, France.*

²*Centre Automatique et Systèmes, Mines-ParisTech,
PSL Research University, 60, bd Saint-Michel, 75006 Paris, France.*

(Dated: July 11, 2021)

We present a twofold contribution to the numerical simulation of Lindblad equations. First, an adaptive numerical approach to approximate Lindblad equations using low-rank dynamics is described: a deterministic low-rank approximation of the density operator is computed, and its rank is adjusted dynamically, using an on-the-fly estimator of the error committed when reducing the dimension. On the other hand, when the intrinsic dimension of the Lindblad equation is too high to allow for such a deterministic approximation, we combine classical ensemble averages of quantum Monte Carlo trajectories and a denoising technique. Specifically, a variance reduction method based upon the consideration of a low-rank dynamics as a control variate is developed. Numerical tests for quantum collapse and revivals show the efficiency of each approach, along with the complementarity of the two approaches.

PACS numbers: 03.65.Yz, 02.60.Cb, 42.50.Pq, 42.50.Md, 02.70.Ss

INTRODUCTION

Lindblad equations are notoriously challenging to simulate numerically. The two categories of approaches are deterministic approaches, on the one hand, and Monte-Carlo approaches [1], on the other hand. Both categories have their pros and cons. In the former category, the simulation is extremely effective when possible, but a major difficulty lies in the high dimensionality of the ambient space which drastically limits the applicability. In the latter category, dimensionality is not an issue, but the intrinsic noise of stochastic simulations affects the quality of the numerical results. The twofold purpose of this article is to present recent advances in either of the two categories of approaches.

In a previous work [2], the first two authors have presented a possible deterministic approach for the simulation of the Lindblad equation, actually borrowed from similar ideas introduced in [3, 4] in the context of quantum filtering. The approach consists in approximating the evolution of the $n \times n$ density matrix ρ solution to the differential Lindblad equation using a reduced dynamics on the set of density matrices of some fixed rank $m \ll n$. This reduced dynamics is obtained by taking the orthogonal projection of $\frac{d}{dt}\rho$ onto the tangent space to this set of rank- m matrices. The clear limitation of the approach lies in the fact that many practical problems are *not* reducible to a low-rank approximation, and further that, even when it is the case, the intrinsic dimensionality of the reduced dynamics is not necessarily known beforehand and may vary in time. So the question of *adjusting* on-the-fly the dimensionality m of the low rank dynamics immediately arises. As our first contribution in the present article, we describe below an *adaptive* low-rank simulation, the purpose of which is

to significantly extend the applicability of the approach introduced earlier in [2]. The questions we examine in this work enjoy some similarity with questions arising in computational quantum chemistry, typically for multi-configuration time-dependent Hartree and Hartree-Fock equations [5, 6].

For problems definitely not amenable to deterministic simulation because of their prohibitively high dimensionality (which is indeed the case for many practically relevant problems), stochastic approaches are in order, *see* [1, 7–9]. Although the low-rank dynamics no longer adequately represents the system, a reduced model, simulated deterministically, can however serve as a useful tool for the stochastic simulation of the high dimensional system. We employ the reduced dynamics as a *control variate* within a variance reduction method applied to the full, high dimensional stochastic system. Our second contribution is to demonstrate the efficiency of such a variance reduction method.

ADAPTIVE LOW-RANK APPROXIMATION

We consider throughout this article a Lindblad equation with, for simplicity (and this is by no means a limitation of our methods), a single decoherence operator L ,

$$\frac{d}{dt}\rho = -i[H, \rho] - \frac{1}{2}(L^\dagger L \rho + \rho L^\dagger L) + L \rho L^\dagger, \quad (1)$$

where ρ is a $n \times n$ non-negative Hermitian matrix with $\text{Tr}(\rho) = 1$, H is a $n \times n$ Hermitian matrix and L is a $n \times n$ matrix. The reduced dynamics derived in [2] approximates, for n large, the above dynamics on the set of non-negative Hermitian matrices of rank m , m being an integer presumably much smaller than n . To make the

approximation explicit, one introduces a system of two coupled differential equations for U and σ corresponding to the generic decomposition $\rho_{\text{LR}} = U\sigma U^\dagger$, where σ is a $m \times m$ strictly positive Hermitian matrix, U a $n \times m$ matrix with $U^\dagger U = \mathbb{I}_m$, and \mathbb{I}_m denotes the $m \times m$ identity matrix. That system reads as:

$$\begin{aligned} \frac{d}{dt}U &= -iHU \\ &+ (\mathbb{I}_n - UU^\dagger) \left(-\frac{1}{2}L^\dagger LU + LU\sigma U^\dagger L^\dagger U\sigma^{-1} \right), \end{aligned} \quad (2)$$

$$\begin{aligned} \frac{d}{dt}\sigma &= -\frac{1}{2}(U^\dagger L^\dagger LU\sigma + \sigma U^\dagger L^\dagger LU) + U^\dagger LU\sigma U^\dagger L^\dagger U \\ &+ \frac{1}{m}\text{Tr} \left(L^\dagger (\mathbb{I}_n - UU^\dagger) L U\sigma U^\dagger \right) \mathbb{I}_m. \end{aligned} \quad (3)$$

Notice that H only appears in (2) and not in (3), a fact that is particularly appropriate when H dominates L , in which case (3) may be understood as a slow evolution as compared to the dynamics (2). Then the projection of the original Lindblad dynamics (1) onto the tangent space to the set \mathcal{D}_m of density matrices of rank m takes the explicit form

$$\begin{aligned} \frac{d}{dt}\rho_{\text{LR}} &= -i[H, \rho_{\text{LR}}] - \frac{1}{2}(L^\dagger L\rho_{\text{LR}} + \rho_{\text{LR}}L^\dagger L) + L\rho_{\text{LR}}L^\dagger \\ &- (\mathbb{I}_n - P_{\rho_{\text{LR}}})L\rho_{\text{LR}}L^\dagger(\mathbb{I}_n - P_{\rho_{\text{LR}}}) \\ &+ \frac{\text{Tr}(L\rho_{\text{LR}}L^\dagger(\mathbb{I}_n - P_{\rho_{\text{LR}}}))}{m}P_{\rho_{\text{LR}}}, \end{aligned} \quad (4)$$

where the orthogonal projection on the image of ρ_{LR} , $P_{\rho_{\text{LR}}} = UU^\dagger$, only depends on ρ_{LR} . Notice that the right-most term of (4) allows $\text{Tr}(\rho_{\text{LR}})$ to be preserved in time. In the sequel, we denote by \mathcal{L} the right-hand side of (1), \mathcal{L}^\parallel that of (4), and by $\mathcal{L}^\perp = \mathcal{L} - \mathcal{L}^\parallel$.

We have described in details in [2] how system (2)-(3) may be efficiently simulated and then provides an accurate approximation of (1) in the case when the rank can be actually reduced. In that work, the rank m was prescribed *beforehand*. Our purpose here is to explain how the approach can be amended so as to allow for a *dynamical adaptation* of the rank m of the reduced system.

The adaptation we suggest is based on the evaluation, and update, of the projection error

$$\begin{aligned} \mathcal{L}^\perp(\rho_{\text{LR}}) &= (\mathbb{I}_n - P_{\rho_{\text{LR}}})L\rho_{\text{LR}}L^\dagger(\mathbb{I}_n - P_{\rho_{\text{LR}}}) \\ &- \frac{\text{Tr}(L\rho_{\text{LR}}L^\dagger(\mathbb{I}_n - P_{\rho_{\text{LR}}}))}{m}P_{\rho_{\text{LR}}} \end{aligned}$$

committed when replacing (1) by (4).

This error may be reduced upon adding one dimension to the m -dimensional subspace $\text{Im}(U)$ associated to the projector $P_{\rho_{\text{LR}}}$. The best possible such dimension to add is that for which the projection error is minimal. The rank- m projector $P_{\rho_{\text{LR}}} = UU^\dagger \in \mathbb{R}^{m \times m}$ is modified into the rank- $m+1$ projector $P_{\rho_{\text{LR}}} + Q = UU^\dagger + VV^\dagger \in \mathbb{R}^{m \times m}$

where $Q = VV^\dagger$, with $V \in \mathbb{R}^n$, is the one-dimensional projector associated to the one dimension added. Denoting by

$$G = (\mathbb{I}_n - P_{\rho_{\text{LR}}})L\rho_{\text{LR}}L^\dagger(\mathbb{I}_n - P_{\rho_{\text{LR}}}),$$

a straightforward calculation yields

$$\begin{aligned} \text{Tr}^2(\mathcal{L}_{P+Q}^\perp(\rho_{\text{LR}})) &= \|(\mathbb{I}_n - Q)G(\mathbb{I}_n - Q)\|^2 \\ &+ \frac{1}{m+1}\text{Tr}^2((\mathbb{I}_n - Q)G). \end{aligned}$$

One may then prove (see the details in [10]) that the directions

$$V = \text{Argmin}_{V \perp U, \|V\|=1} \|\mathcal{L}_{P_{\rho_{\text{LR}}} + Q}^\perp(\rho_{\text{LR}})\| \quad (5)$$

minimizing the projection error are the eigenvectors of the symmetric matrix G associated to its largest eigenvalue. The matrix G being of large size n , determining its largest eigenvector is challenging computationally. To this end, we notice that

$$V^\dagger G V = \|V^\dagger(\mathbb{I}_n - P_{\rho_{\text{LR}}})LU\sqrt{\sigma}\|^2,$$

and that the range of $(\mathbb{I}_n - P_{\rho_{\text{LR}}})LU$ is of dimension less or equal to m and is orthogonal to the range of ρ_{LR} . Thus, denoting by $(\phi_j)_{0 \leq j < r}$ an orthonormal basis of the range of $(\mathbb{I}_n - P_{\rho_{\text{LR}}})LU$ with $r \leq m$, it is sufficient to consider V as linear combination of the ϕ_j to get an eigenvector of G with largest eigenvalue: $V = \sum_{j=1}^r v_j \phi_j$ where the r -dimensional vector v of component v_j corresponds to the eigenvector with largest eigenvalue of

$$K = \Phi^\dagger(\mathbb{I}_n - P_{\rho_{\text{LR}}})L\rho_{\text{LR}}L^\dagger(\mathbb{I}_n - P_{\rho_{\text{LR}}})\Phi,$$

with Φ the $n \times r$ matrix formed by the r vectors ϕ_j . Since K is of size $r \leq m$, this provides an effective manner to determine the optimum in (5).

We have performed a comprehensive series of test of the approach. The practical implementation of the dynamical adaptivity of the rank is performed as follows.

We denote by $\theta(\rho_{\text{LR}}) \equiv \frac{\|\mathcal{L}^\perp(\rho_{\text{LR}})\|}{\|\mathcal{L}^\parallel(\rho_{\text{LR}})\|}$, fix a maximal angular error θ_{max} and update the rank

- increasing m by 1, when $\theta(\rho_{\text{LR}}) > \theta_{\text{max}}$ and then complementing U via the solution of (5);
- reducing m by 1, when the smallest eigenvalue λ_{min} of σ is such that $\theta(\rho_{\text{LR}}) + \lambda_{\text{min}} < \frac{1}{2}\theta_{\text{max}}$.

As an illustrative example, we consider a qubit resonantly coupled to a quantized harmonic damped oscillator:

$$\frac{d}{dt}\rho = \frac{\Omega_0}{2}[\mathbf{a}^\dagger \boldsymbol{\sigma}_- - \mathbf{a}\boldsymbol{\sigma}_+, \rho] - \kappa(\mathbf{n}\rho/2 + \rho\mathbf{n}/2 - \mathbf{a}\rho\mathbf{a}^\dagger), \quad (6)$$

with $\Omega_0 > 0$ the vacuum Rabi pulsation, \mathbf{a} the photon annihilation operator, $\boldsymbol{\sigma}_-$ the qubit lowering operator

($\sigma_- = |g\rangle\langle e|$), $\sigma_+ = \sigma_-^\dagger$, $\mathbf{n} = \mathbf{a}^\dagger \mathbf{a}$ the photon-number operator and $1/\kappa > 0$ the oscillator damping time. In Figure 3.20, page 156 of [9], numerical simulations of quantum collapse and revivals are presented, for $\kappa = 0$, when the qubit is initially in the excited state $|e\rangle$ and the oscillator in a coherent state with $\bar{n} = 15$ photons. We consider here the same system with $\kappa = \Omega_0/500$, a value small compared to Ω_0 . This corresponds to a photon life-time $1/\kappa$ around 10 times as large as the revival time $T_r = \frac{4\pi\sqrt{\bar{n}}}{\Omega_0}$. In this simple case, we can perform the full-rank simulation with high precision. This simulation illustrated on Figure (1) provides us with a reference calculation. As shown in [2], a constant rank of 4 is sufficient to compute accurately the solution $t \mapsto \rho_t$ for t between 0 and $2T_r$. For intermediate values of t , larger than $2T_r$ but not excessively larger, the quantum state ρ gets more and more mixed. For t very large, ρ becomes again pure, since its limit for $t \mapsto +\infty$ is the lowest energy state (qubit in the ground state $|g\rangle$, oscillator with zero photon). This behavior, illustrated by the numerical simulations of Figure 2, is well captured by our adaptive approach.

DENOISED MONTE-CARLO APPROACH

In the case when the Lindblad equation (1) is genuinely high-dimensional, the model reduction previously described is likely to be either ineffective or inaccurate, while the direct integration of the equation is out of reach. In this situation, the classical approach is to use a Monte-Carlo sampling. One derives a stochastic dynamics on the wave function $|\psi_t\rangle$ such that the density $\rho(t) = \mathbb{E}(|\psi_t\rangle\langle\psi_t|)$ constructed from $|\psi_t\rangle$ (\mathbb{E} stands for expectation value, i.e. ensemble average) solves the Lindblad equation (1). In practice, M independent trajectories, $|\psi_t^{(k)}\rangle$ with $k = 1, \dots, M$, are then simulated using that stochastic dynamics and the estimator of the mean

$$\bar{\rho}_{\text{MC}}(t) = \frac{1}{M} \sum_{k=1}^M \left| \psi_t^{(k)} \right\rangle \left\langle \psi_t^{(k)} \right| \quad (7)$$

is used as an approximation of $\rho(t)$. The practical difficulty of Monte-Carlo approaches is, as briefly mentioned, above, the variance, that is, the noise intrinsically present in the approach.

In principle, there are infinitely many dynamics on $|\psi_t\rangle$ that are consistent with the Lindblad dynamics. Interestingly, a straightforward calculation from (7) shows that

$$\mathbb{E} \left(\text{Tr} \left((\bar{\rho}_{\text{MC}} - \rho)^2 \right) \right) = \frac{1 - \text{Tr}(\rho^2)}{M}. \quad (8)$$

The variance of the estimator of the mean $\bar{\rho}_{\text{MC}}$ is therefore independent of the specific unravelling choice, namely the stochastic dynamics set on $|\psi_t\rangle$, provided that

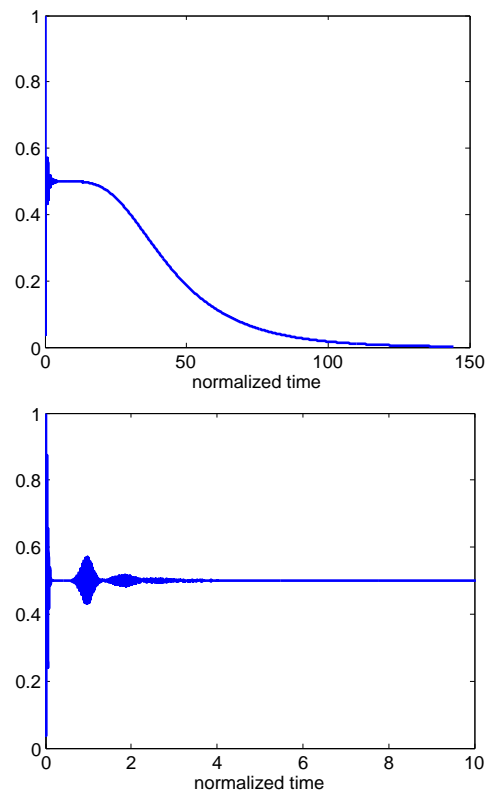


FIG. 1. (color online) High precision full-rank numerical simulation of $t \mapsto \rho(t)$ for the quantum collapse and revivals of a qubit resonantly coupled to a slightly damped quantum harmonic oscillator governed by (6). Top plot: the solid curve corresponds to the excited population $\langle e|\rho|e\rangle$ versus time; the normalized time corresponds to t/T_r where T_r is the revival time; the oscillator damping time is around $10T_r$; the initial state ρ_0 corresponds to the qubit in excited state $|e\rangle$ and oscillator in a coherent state with $\bar{n} = 15$ photons; a truncation of the number of photons to a maximum of $2\bar{n} = 30$ yields an underlying Hilbert space of dimension 62. Bottom plot: zoom of top plot for a normalized time between 0 and 10.

state $|\psi_t\rangle$ remains normalized. This is easily seen in the proof of (8). This property is, of course, a remarkable peculiarity of the present context. And the discretization in time of the process can of course slightly affect that property. The classical unravelling choice (see [11–13]) is the Wiener process defined by

$$d|\psi_t\rangle = D_1(|\psi_t\rangle) dt + D_2(|\psi_t\rangle) dW_t, \quad (9)$$

with the drift term

$$\begin{aligned} D_1(|\psi\rangle) &= -iH|\psi\rangle + D_1^0(|\psi\rangle) \quad \text{where} \\ D_1^0(|\psi\rangle) &= \frac{1}{2} \left(\langle L + L^\dagger \rangle_{|\psi\rangle} L - L^\dagger L - \frac{1}{4} \langle L + L^\dagger \rangle_{|\psi\rangle}^2 \right) |\psi\rangle, \end{aligned} \quad (10)$$

and the diffusion

$$D_2(|\psi\rangle) = \left(L - \frac{1}{2} \langle L + L^\dagger \rangle_{|\psi\rangle} \right) |\psi\rangle. \quad (11)$$

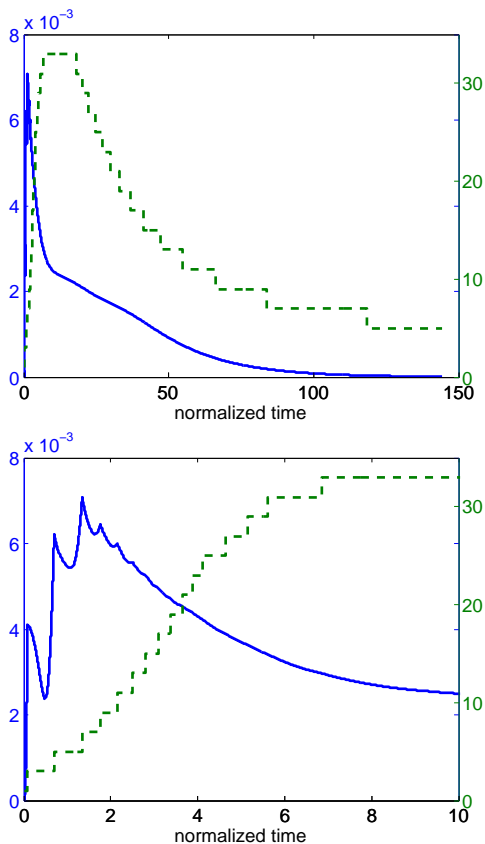


FIG. 2. (color online) Comparison between the full-rank trajectory $t \mapsto \rho(t)$ illustrated on figure 1 with the adaptive rank trajectory $t \mapsto \rho_{\text{LR}}(t)$ governed by (2-3). Top plot: the solid curve corresponds to $\sqrt{\text{Tr}((\rho - \rho_{\text{LR}})^2)}$ versus time with scale on the left. The dashed curve corresponds to the adaptive rank m with scale on the right; the initial low rank state ρ_{LR} coincides with ρ_0 ; the initial rank m is thus set to one; it evolves according to the maximal angular error $\theta_{\text{max}} = \frac{1}{1000}$. Bottom plot: zoom of top plot for a normalized time between 0 and 10.

We have used the notation $\langle A \rangle_{|\psi\rangle} = \langle \psi | A | \psi \rangle$. We emphasize that other choices of dynamics on $|\psi\rangle$, all consistent with the Lindblad equation through $\rho(t) = \mathbb{E}(|\psi_t\rangle \langle \psi_t|)$, could be made. In particular, Poisson processes could be considered instead of Wiener processes (a choice that can be seen as more natural given the applications addressed in the present work where photons are emitted or absorbed). In any event, given the property (8) and assuming that the Poisson process remains normalized, the variance remains identical. We indeed double-checked that, in actuality, using Poisson processes does not bring further practical variance reduction, see [10] for more details.

Variance is an issue for the numerical simulation and affects the accuracy of the results. It is thus desirable to come up with further, dedicated variance reduction approaches that may reduce the computational cost at accuracy fixed, or improve the accuracy for a given com-

putational cost. An approach that has proved effective in many engineering sciences for reducing variance of Monte-Carlo simulations is that of *control variate*, see e.g. [14, page 54]. In short, the approach consists in *concurrently* simulating the original system under consideration and a system *correlated* to that original system so as to minimize the variance in the simulation of the former system. Intuitively, the approach works by "cancellation" of the noise because the same random draws are used for both systems. More specifically, we consider here as control variate the low-rank approximation ρ_{LR} of previous section. Even though that low-rank system is not a correct approximation of the original system (which we have deliberately assumed here high-dimensional), it is sufficiently correlated to that system to provide an efficient variance reduction. Practically, we construct an ("Control-Variate") estimated density depending on the adjustable scalar parameter λ ,

$$\bar{\rho}_{\text{CV}} = \bar{\rho}_{\text{MC}} + \lambda(\rho_{\text{LR}} - \bar{\rho}_{\text{MCLR}}), \quad (12)$$

as a combination of the original Monte-Carlo estimated density $\bar{\rho}_{\text{MC}}$ (constructed from the simulation of (7)-(9)), the estimated density $\bar{\rho}_{\text{MCLR}}$ constructed from a low-rank dynamics ("Monte-Carlo-Low-Rank", see below (13)), and the density ρ_{LR} obtained upon solving the corresponding low-rank Lindblad equation. Since by construction

$$\mathbb{E}[\bar{\rho}_{\text{MCLR}}(t)] = \rho_{\text{LR}}(t),$$

the approximation method (12) is unbiased (taking the expectation of both sides of (12) yields $\rho = \mathbb{E}[\bar{\rho}_{\text{CV}}] = \mathbb{E}[\bar{\rho}_{\text{MC}}]$). The scalar parameter λ is adjusted so as to minimize the variance $\mathbb{E}(\text{Tr}((\bar{\rho}_{\text{CV}} - \rho)^2))$, a polynomial in λ of degree 2, in such a way that

$$\mathbb{E}(\text{Tr}((\bar{\rho}_{\text{CV}} - \rho)^2)) \ll \mathbb{E}(\text{Tr}((\bar{\rho}_{\text{MC}} - \rho)^2))$$

so that the simulation of $\bar{\rho}_{\text{CV}}$ is eventually more effective than that of $\bar{\rho}_{\text{MC}}$. The more correlated the reduced model and the original model, the closer λ to one, the smaller this variance and thus the more efficient the denoising. In passing, we notice that, although this will not be the case in the actual numerical experiments we perform, the low-rank dynamics $\rho_{\text{LR}}(t)$ could itself be chosen with an adaptive rank, as in the previous section. Likewise, we could pick as control variate another dynamics than the low-rank dynamics, if a more convenient one is available.

The remaining question is to derive a stochastic dynamics on a wave function $|\psi_{\text{LR}}\rangle$ such that $\mathbb{E}(|\psi_{\text{LR}}\rangle \langle \psi_{\text{LR}}|) = \rho_{\text{LR}}$, given that the dynamics of ρ_{LR} is known since easy to compute via (U, σ) solutions of (2) and (3). For this purpose, it is a natural idea to seek $|\psi_{\text{LR}}\rangle$ under the form $|\psi_{\text{LR}}\rangle = U|\nu\rangle$ where the reduced wave

function $|\nu\rangle \in \mathbb{R}^m$ is a stochastic process to be determined. It can be shown (see [10]) that the correct dynamics to consider reads

$$\begin{aligned} d|\psi_{\text{LR}}\rangle &= P_{\rho_{\text{LR}}} D_1(|\psi_{\text{LR}}\rangle) dt + P_{\rho_{\text{LR}}} D_2(|\psi_{\text{LR}}\rangle) dW_t \\ &+ (\mathbb{I}_n - P_{\rho_{\text{LR}}}) \left(-\frac{1}{2} L^\dagger L + LU\sigma U^\dagger L^\dagger U\sigma^{-1} U^\dagger \right) |\psi_{\text{LR}}\rangle dt \\ &+ \frac{\text{Tr}((\mathbb{I}_n - P_{\rho_{\text{LR}}})L\rho_{\text{LR}}L^\dagger)}{2m} U\sigma^{-1} U^\dagger |\psi_{\text{LR}}\rangle dt, \end{aligned} \quad (13)$$

with D_1 and D_2 defined in (10) and (11).

Since $\bar{\rho}_{\text{MCLR}} = \frac{1}{M} \sum_{k=1}^M |\psi_{\text{LR}}^{(k)}\rangle \langle \psi_{\text{LR}}^{(k)}|$, a simple computation, exploiting the fact that both $|\psi^{(k)}\rangle$ and $|\psi_{\text{LR}}^{(k)}\rangle$ are normalized, shows that

$$\begin{aligned} M \mathbb{E} \left(\text{Tr} \left((\bar{\rho}_{\text{CV}} - \rho)^2 \right) \right) &= (1 - \text{Tr}(\rho_{\text{LR}}^2)) \lambda^2 \\ &+ 2 \left(\mathbb{E} \left(|\langle \psi | \psi_{\text{LR}} \rangle|^2 \right) - \text{Tr}(\rho \rho_{\text{LR}}) \right) \lambda + 1 - \text{Tr}(\rho^2). \end{aligned}$$

Thus the optimal denoising choice for λ reads

$$\lambda = \frac{\text{Tr}(\rho \rho_{\text{LR}}) - \mathbb{E} \left(|\langle \psi | \psi_{\text{LR}} \rangle|^2 \right)}{1 - \text{Tr}(\rho_{\text{LR}}^2)}. \quad (14)$$

In practice, *and also* in the simulations of Figure (3), the adjustable parameter λ is given by (14) where the ρ is replaced by $\bar{\rho}_{\text{MC}}$ (we do not have access to ρ itself) and where $\mathbb{E} \left(|\langle \psi | \psi_{\text{LR}} \rangle|^2 \right)$ is replaced by the estimated mean $\frac{1}{M} \sum_{k=1}^M \left| \langle \psi^{(k)} | \psi_{\text{LR}}^{(k)} \rangle \right|^2$.

Figure (3) illustrates the interest of this denoising method for the Lindblad system simulated in Figure (2). We take $M = 400$ trajectories. The dynamics of $|\psi_{\text{LR}}\rangle$ is based on a low-rank approximation ρ_{LR} of constant rank $m = 2$. On the bottom plot of Figure 2, we observe that, at normalized time 2, an accurate approximation of ρ must be of rank 10 or larger. Nevertheless, Figure 3 indicates that, at normalized time 2, a reduction of the standard deviation around 50% is obtained with $\bar{\rho}_{\text{CV}}$ instead of $\bar{\rho}_{\text{MC}}$. Such a variance reduction corresponds, with a classical quantum Monte-Carlo method, to an increase of the number of trajectories by a factor 4. Such a gain confirms the definite interest of combining deterministic low-rank approximations with quantum Monte-Carlo trajectories for the numerical simulation of high-dimensional Lindblad equation.

ACKNOWLEDGMENTS

The first two authors are partially supported by the ANR, Projet Blanc EMAQS ANR-2011-BS01-017-01.

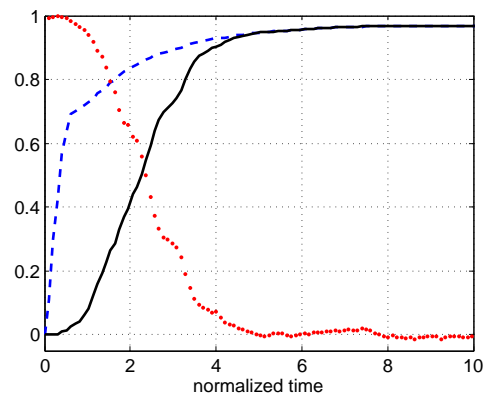


FIG. 3. (color online) Variance reduction corresponding to the quantum collapse and revivals in the bottom plot of Figure 2. The solid black curve corresponds to $\sqrt{\text{Tr}((\rho - \bar{\rho}_{\text{CV}})^2)}$, the dashed blue one to $\sqrt{\text{Tr}((\rho - \bar{\rho}_{\text{MC}})^2)}$ and the dotted red one to λ . The number of trajectories M is set to 400. The low-rank approximation ρ_{LR} used for the control variate governed by (13) is maintained at the constant rank $m = 2$.

* pierre.rouchon@mines-paristech.fr

- [1] J. Dalibard, Y. Castin, and K. Mølmer, *Phys. Rev. Lett.* **68**, 580 (1992).
- [2] C. Le Bris and P. Rouchon, *Phys. Rev. A* **87**, 022125 (2013).
- [3] R. v. Handel and H. Mabuchi, *Journal of Optics B: Quantum and Semiclassical Optics* **7**, S226 (2005).
- [4] H. Mabuchi, *Phys. Rev. A* **78**, 015801 (2008).
- [5] C. Lubich, *From quantum to classical molecular dynamics: reduced models and numerical analysis*, Zurich Lectures in Advanced Mathematics (European Mathematical Society (EMS), Zürich, 2008) pp. x+144.
- [6] C. Lubich and I. V. Oseledets, *BIT* **54**, 171 (2014).
- [7] K. Mølmer, Y. Castin, and J. Dalibard, *J. Opt. Soc. Am. B* **10**, 524 (1993).
- [8] Y. Castin and K. Mølmer, *Phys. Rev. Lett.* **74**, 3772 (1995).
- [9] S. Haroche and J. Raimond, *Exploring the Quantum: Atoms, Cavities and Photons*. (Oxford University Press, 2006).
- [10] J. Roussel, *Numerical simulation of high dimensional open quantum systems (in French)*, *Master's thesis*, Univ. Pierre et Marie Curie, Laboratoire J.L. Lions, <https://hal.inria.fr/hal-01205747> (2015).
- [11] N. Gisin and I. C. Percival, *Journal of Physics A: Mathematical and General* **25**, 5677 (1992).
- [12] H.-P. Breuer and F. Petruccione, *The Theory of Open Quantum Systems* (Clarendon-Press, Oxford, 2006).
- [13] A. Barchielli and M. Gregoratti, *Quantum Trajectories and Measurements in Continuous Time: the Diffusive Case* (Springer Verlag, 2009).
- [14] C. Graham and D. Talay, *Stochastic simulation and Monte Carlo methods*, Stochastic Modelling and Applied Probability, Vol. 68 (Springer, Heidelberg, 2013) pp. xvi+260.